

Ring current effects on nuclear magnetic shielding of carbon in the benzene molecule

M. B. Ferraro,¹ F. Faglioni,² A. Ligabue,² S. Pelloni² and P. Lazzeretti^{2*}

¹ Departamento de Física, Facultad de Ciencias Exactas y Naturales, Universidad de Buenos Aires, Ciudad Universitaria, Pab. I, (1428) Buenos Aires, Argentina

² Dipartimento di Chimica dell'Università degli Studi di Modena e Reggio Emilia, Via Campi 183, 41100 Modena, Italy

Received 28 August 2004; Revised 27 October 2004; Accepted 8 November 2004

The differential Biot–Savart law of classical electrodynamics was applied to develop a ring current model for the magnetic shielding of the carbon nucleus in benzene. It is shown that the local effect of the π currents, induced by a magnetic field normal to the molecular plane, on the σ_{\parallel}^C out-of-plane shielding tensor component vanishes. However, approximately 10% of σ_{\parallel}^C is due to the shielding contributions from π current density in the region of the other carbon atoms. Magnetic shielding density maps obtained via quantum mechanical procedures confirm the predictions of the classical model. Copyright © 2005 John Wiley & Sons, Ltd.

KEYWORDS: NMR; ring current; magnetic shielding; carbon; benzene; differential Biot–Savart law

INTRODUCTION

The magnetic shielding tensor of carbon nuclei in arenes is strongly anisotropic. In the benzene molecule, the experimental value¹ of the anisotropy $\Delta\sigma^C = \sigma_{\parallel}^C - \sigma_{\perp}^C$ is 180 ± 5 ppm, with the out-of-plane component $\sigma_{\parallel}^C \equiv \sigma_{zz}^C$ and the average in-plane component $\sigma_{\perp}^C = (1/2)(\sigma_{xx}^C + \sigma_{yy}^C)$ being as large as 186 ppm (in agreement with the value of 190 in Ref. 2) and 6 ppm, respectively. The experimental average shielding $\sigma_{Av}^C = (1/3)(\sigma_{xx}^C + \sigma_{yy}^C + \sigma_{zz}^C)$ is 57.2 ppm.³

The mechanism causing this unusually strong anisotropy is not fully understood. In particular, a possible role of the ring currents, induced in the π electrons by a uniform static magnetic field perpendicular to the molecular plane of benzene, has not been ascertained so far.^{4,5} The ring currents enhance the out-of-plane component of the susceptibility tensor $\chi_{\alpha\beta}$ and lower the value of the out-of-plane component of magnetic shielding σ_{\parallel}^H of the protons, determining a downfield (paramagnetic) shift, i.e. deshielding.^{4–8}

Recent discussions^{8–10} reinforced the conviction that only the out-of-plane components of magnetic response tensors of arenes are biased by the π ring currents. A mere analysis of average values, e.g. $(1/3)\sigma_{\alpha\alpha}^H$, causes a loss of information (two-thirds of the deshielding due to ring currents), introduces spurious contributions from mixed σ

and π electron flow induced by a magnetic field parallel to the molecular plane and leads to serious errors.

It is usually accepted that the local effect on a C nucleus, carrying the probe magnetic dipole μ_C , exerted by the π diamagnetic ring currents in which it is immersed, vanishes, since, according to the Biot–Savart law, the induced magnetic field changes sign on crossing the current stream.⁴ However, there is theoretical evidence for a π -electron biased effect on nuclear shielding of benzene carbon. The π electron contribution to σ_{\parallel}^C , estimated by common-origin coupled Hartree–Fock (CHF) calculations (see Table 11 in Ref. 5), is ~ 19 ppm, that is, 10% of the total out-of-plane component of carbon nuclear shielding. In fact, contributions from distant portions of the π ring currents cannot be neglected to develop a model for rationalizing carbon magnetic shielding of arenes^{11–13} (see below) (the notion, based on the DBS law, that ¹H and ¹³C shielding-density maps contain signatures of global ring currents, was set out in Ref. 11 for three typical aromatic, non-aromatic and anti-aromatic systems).

RING CURRENT MODELS FROM THE DIFFERENTIAL BIOT–SAVART LAW

The differential Biot–Savart (DBS) relationship¹⁴ provides an insight into the problem. If $d\mathbf{l}$ is an element of length in the direction of current flow in a filament carrying a current I , and \mathbf{r} is the vector from $d\mathbf{l}$ to an observation point P , then the elemental flux density $d\mathbf{B}_{\text{ind}}$ at P is obtained as

$$d\mathbf{B}_{\text{ind}}(\mathbf{r}) = \frac{1}{c} \mathbf{J}^{\mathbf{B}} \times \frac{\mathbf{r}}{|\mathbf{r}|^3} dV = -\boldsymbol{\Sigma}(\mathbf{r}) \cdot \mathbf{B} dV \quad (1)$$

where we have used the familiar definition for the current $I = dq/dt$, the element of charge contained in the volume element dV is expressed via the density ρ , i.e., $dq = \rho dV$,

*Correspondence to: P. Lazzeretti, Dipartimento di Chimica dell'Università degli Studi di Modena e Reggio Emilia, Via Campi 183, 41100 Modena, Italy. E-mail: lazzeret@chi02.unimo.it

Contract/grant sponsor: Proyecto del Programa de Cooperación Argentino–Italiana SECYT-MAE; Contract/grant number: IT/PA03-EXII/082.

Contract/grant sponsor: Ministero dell'Università e della Ricerca Scientifica e Tecnologica (MURST).

Contract/grant sponsor: University of Buenos Aires;

Contract/grant number: UBACYT X-035.

Contract/grant sponsor: CONICET.

1 and the current density is $\mathbf{J} = \rho\mathbf{v}$, with $\mathbf{v} = d\mathbf{r}/dt$ the local
2 velocity. We assume that the current density is generated by
3 an external homogeneous and time-independent magnetic
4 field with flux density \mathbf{B} , so that $\mathbf{J} \equiv \mathbf{J}^{\mathbf{B}}$, and $I d\mathbf{l} = \mathbf{J}^{\mathbf{B}} dV$.

5 The second identity in Eqn (1) defines the Jame-
6 son–Buckingham magnetic shielding density tensor^{15,16} at
7 the point P :

$$\Sigma_{\alpha\delta}(\mathbf{r}) = \frac{1}{c} \varepsilon_{\alpha\beta\gamma} \frac{r_{\beta}}{|\mathbf{r}|^3} \mathcal{J}_{\gamma}^{\mathbf{B}_{\delta}} \quad (2)$$

8 The Einstein convention for summing over repeated Greek
9 indices is used throughout this paper, $\varepsilon_{\alpha\beta\gamma}$ is the Levi–Civita
10 tensor and the second-rank current density tensor¹⁷ is the
11 derivative of the current density with respect to the applied
12 field, $\mathcal{J}_{\gamma}^{\mathbf{B}_{\delta}} = \partial \mathbf{J}_{\gamma}^{\mathbf{B}} / \partial B_{\delta}$.

13 The simple Eqn (1) is sufficient to develop a model for
14 understanding the effect of ring currents on the out-of-plane
15 component of the magnetic shielding at the observation
16 point, that is, to determine the sign of the elemental magnetic
17 flux density $d\mathbf{B}_{\text{ind}}$ at P .^{11–13}

18 For instance, it can be used to predict the sign of the
19 contributions to the out-of-plane component of the shielding
20 density in Eqn (2) at a given carbon nucleus, generated by
21 an elemental current $\mathbf{J}^{\mathbf{B}} dV$, for dV placed anywhere along
22 the π current loop.

23 Let us consider a reference carbon nucleus C immersed
24 in the π stream (see Fig. 1). An observer at C , looking in
25 the direction of the diamagnetic current density $\mathbf{J}^{\mathbf{B}}$, and
26 evaluating the effect of the streamline D on his or her
27 right (L on his or her left), at a small distance $r_{\text{D}}(\mathbf{r}_{\text{L}})$,
28 will experience an induced elemental magnetic flux density
29 $d\mathbf{B}_{\text{D}} \propto \mathbf{J}^{\mathbf{B}} \times \mathbf{r}_{\text{D}} / |\mathbf{r}_{\text{D}}|^3 dV (d\mathbf{B}_{\text{L}} \propto \mathbf{J}^{\mathbf{B}} \times \mathbf{r}_{\text{L}} / |\mathbf{r}_{\text{L}}|^3 dV)$, reinforcing
30 (opposing) the external field \mathbf{B}_{ext} . Since the streamlines D and
31 L are close to each other, the current density $\mathbf{J}^{\mathbf{B}}(\mathbf{r}_{\text{D}}) \approx \mathbf{J}^{\mathbf{B}}(\mathbf{r}_{\text{L}})$.
32 In the limit for \mathbf{r}_{D} and $\mathbf{r}_{\text{L}} \rightarrow \mathbf{0}$, that is, at the site of the probe,
33 the magnetic shielding density diverges to $\pm\infty$, because
34 of the r^{-3} factor in the DBS law. In practice, the opposing
35 elemental fields cancel out at the position of μ_{C} , then the ring
36 currents do not have a local effect on $\sigma_{\parallel}^{\text{C}}$.^{4,5}

37 On the other hand, according to the DBS law [Eqn (1)],
38 any other segment of the π current density stream provides
39 an elemental contribution $d\mathbf{B}_{\text{ind}}$ opposing \mathbf{B}_{ext} at the site
40 of the probe, observe, for instance, the circumferences with
41 diameter A – D and F – L in Fig. 1. However, to illustrate
42 this point, it is sufficient to analyze the situation along a
43 single circuit passing through the reference carbon nucleus.
44 The model can be improved supposing that the π currents
45 flow in two loops, one some distance above and the other
46 the same distance below, the molecular plane.^{18,19} A further
47 refinement was proposed by Farnum and Wilcox via a double
48 toroidal model.²⁰ If a loop above the plane is considered, the
49 coordinate vector \mathbf{r} can be resolved into two components, one
50 of them lying in the plane of the current loop. Equation (1)
51 is then applied to this component. It is immediately seen
52 that, with the exception of the discontinuity (in practice, a
53 nodal point) at C , any other portion of the loop carrying
54 the π current yields a $d\mathbf{B}_{\text{ind}}$ contribution which lowers the
55 external magnetic field in the vicinity of the probe μ_{C} , since
56 the vector product $\mathbf{J}^{\mathbf{B}} \times \mathbf{r}$ in Eqn (1) depends on the sine of
57 the angle between these vectors, which is always negative.

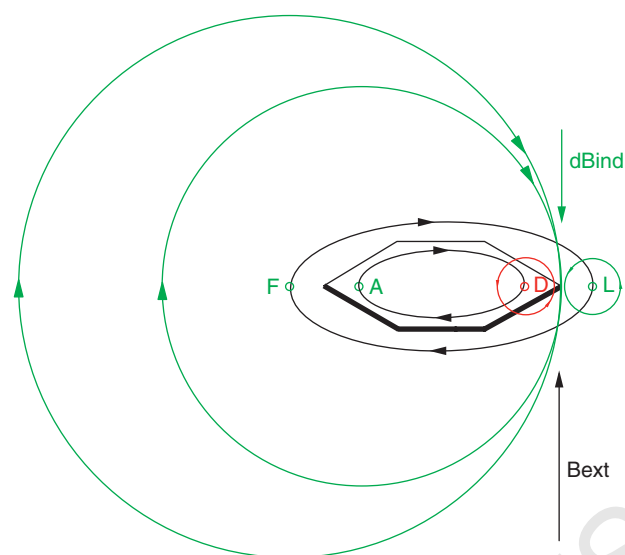


Figure 1. The ring current model for ¹³C magnetic shielding in benzene. The external magnetic field \mathbf{B}_{ext} perpendicular to the molecular xy plane induces a diamagnetic current density in the π electrons. The Biot–Savart magnetic field densities generated by the elemental π currents $\mathbf{J}^{\mathbf{B}}(\mathbf{r}_{\text{D}})dV$ and $\mathbf{J}^{\mathbf{B}}(\mathbf{r}_{\text{L}})dV$ are represented respectively by red and green lines. They cancel each other in the vicinity of the nucleus of carbon C at \mathbf{R}_{C} (see text). The contributions $\mathbf{J}^{\mathbf{B}}(\mathbf{r})dV$, for any point $\mathbf{r} \neq \mathbf{R}_{\text{C}}$ along the circuit through \mathbf{R}_{C} , diminish the external field at C , and cause shielding by increasing the out-of-plane component σ_{zz}^{C} . The shielding effect is represented by the green lines for the elemental $d\mathbf{B}_{\text{ind}}$ from $\mathbf{J}^{\mathbf{B}}(\mathbf{r}_{\text{A}})dV$ and $\mathbf{J}^{\mathbf{B}}(\mathbf{r}_{\text{F}})dV$, for two points, \mathbf{r}_{A} and \mathbf{r}_{F} , on the furthest portion of the ring.

MAGNETIC SHIELDING DENSITY TENSOR

The total effective field induced at the carbon nucleus, with position \mathbf{R}_{C} , is the sum of the elemental contributions [Eqn (1)]. It is evaluated by the integral Biot–Savart (IBS) law:^{14,21}

$$\mathbf{B}_{\text{ind}}(\mathbf{R}_{\text{C}}) = \frac{1}{c} \int \mathbf{J}^{\mathbf{B}}(\mathbf{r}) \times \frac{\mathbf{R}_{\text{C}} - \mathbf{r}}{|\mathbf{R}_{\text{C}} - \mathbf{r}|^3} d^3r \equiv -\sigma(\mathbf{R}_{\text{C}}) \cdot \mathbf{B} \quad (3)$$

In this expression, the current density is a vector field, explicitly depending on the coordinate \mathbf{r} , which gives the distance of the volume element d^3r from the origin. The total effective field acting on the probe is $\mathbf{B} + \mathbf{B}_{\text{ind}}(\mathbf{R}_{\text{C}})$, where the second-rank dimensionless tensor $\sigma(\mathbf{R}_{\text{C}})$ defines the local magnetic shielding. The magnetic shielding is defined via^{17,21}

$$\sigma_{\alpha\beta}(\mathbf{R}_{\text{C}}) \equiv \sigma_{\alpha\beta}^{\text{C}} = \int d^3r \Sigma_{\alpha\beta}^{\text{C}}(\mathbf{r}) \quad (4)$$

using the explicit form for the shielding density of the reference carbon nucleus:

$$\Sigma_{\alpha\delta}^{\text{C}}(\mathbf{r}) = -\frac{1}{c} \varepsilon_{\alpha\beta\gamma} \frac{r_{\beta} - R_{\text{C}\beta}}{|\mathbf{r} - \mathbf{R}_{\text{C}}|^3} \mathcal{J}_{\gamma}^{\mathbf{B}_{\delta}}(\mathbf{r}) \quad (5)$$

This quantity is a non-symmetric second-rank tensor function of position in three-dimensional space, with the dimension of the inverse of a volume. Its connection with the quantities appearing in the DBS law are explicit from Eqns (1) and (5).

1 There is a one-to-one correspondence between the $J_a^B(\mathbf{r})$ and
 2 $\Sigma_{\alpha\beta}^C(\mathbf{r})$ fields, which provide complementary information on
 3 molecular magnetic response.

4 The components of $\Sigma_{\alpha\beta}^C$ can be plotted over a plane
 5 specified by fixing one coordinate. The shielding density
 6 function is useful to determine the regions of the molecular
 7 basin where shielding–deshielding mechanisms are at work,
 8 and to analyze the contribution provided by different
 9 domains of the $J^B(\mathbf{r})$ field.^{7,15,16,22,23}

10 To check the reliability of the predictions for the π ring
 11 current contributions to carbon magnetic shielding in arenes
 12 based on the DBS Eqn (1), the shielding density $\Sigma_{zz}^C(\mathbf{r})$ was
 13 evaluated for the benzene molecule in the presence of a
 14 magnetic field at right angles to the molecular xy plane.
 15 A non-contracted (13s10p5d2f/8s4p1d) basis set,²⁴ with 714
 16 primitive Gaussian functions, was used within the approach
 17 of continuous transformation of the origin of the current
 18 density–diamagnetic zero (CTOCD-DZ),^{5,17} allowing for the
 19 CHF approximation.²⁵ The damped DZ2^{26,27} procedure was
 20 adopted for carbon shielding. The experimental geometry
 21 quoted in Ref. 28, $r_{CC} = 1.395 \text{ \AA}$, $r_{CH} = 1.085 \text{ \AA}$, was
 22 employed. The values of the magnetic shielding components
 23 calculated via the 714 Gaussian-type orbital basis set are
 24 $\sigma_{\perp}^C = -14.68 \text{ ppm}$, $\sigma_{\parallel}^C = 184.98 \text{ ppm}$ and $\sigma_{Av}^C = 51.87 \text{ ppm}$.
 25 The π -electron contribution to σ_{\parallel}^C is as large as 18.73 ppm.
 26 The magnetic shielding density maps are shown in Figs 2–5.

27 MAPS OF MAGNETIC SHIELDING DENSITY

28 To avoid divergence problems, which may occur because
 29 of the overall r^{-2} dependence of the elemental induced
 30 flux density in Eqn (1), the plane of the plot in Fig. 2 was
 31 chosen at a distance of 0.05 bohr above that of the molecule,
 32 which is a nodal plane for π electrons. In low resolution,
 33 the figure shows a very sharp spike-up centered over the
 34 carbon nucleus, corresponding to an intense diamagnetic
 35 vortex observable in the current density map (see Fig. 4 in
 36 Ref. 5). Therefore, the unusually high value of the out-of-
 37 plane carbon shielding is due essentially to core and, in part,
 38 to σ electrons. By expanding the scale of the plot, it can
 39 be seen that the diamagnetic vortices about the other carbon
 40 nuclei give rise to shielding and deshielding spikes of similar
 41 magnitude, making contributions to σ_{\parallel}^C that effectively cancel
 42 each other.

43 Plots of shielding density in planes at increasing distances
 44 from the molecular plane illustrate a dramatic fall-off of the
 45 shielding density at the carbon nucleus. The plot planes in
 46 Figs 3 and 4 pass through a region of high π electron density.
 47 The contributions provided by core and σ electrons can be
 48 observed on top of the figures. They are orders of magnitude
 49 smaller than those on the molecular plane. The spike-up,
 50 spike-down pair in the vicinity of the carbon nucleus, and
 51 the chain of shielding peaks, observed in the central plots for
 52 π electrons, is exactly that predicted via the DBS law (see the
 53 second section). The different height of the peaks depends
 54 on the overall r^{-2} factor in the shielding density [Eqn (5)]
 55 and on the non-uniformity of the modulus of the π current
 56 above the nuclei and the bond regions.

57 The pattern observable for the plot plane $z = 1.5 \text{ bohr}$
 58 (Fig. 5) is qualitatively the same as that in Figs 3 and 4.

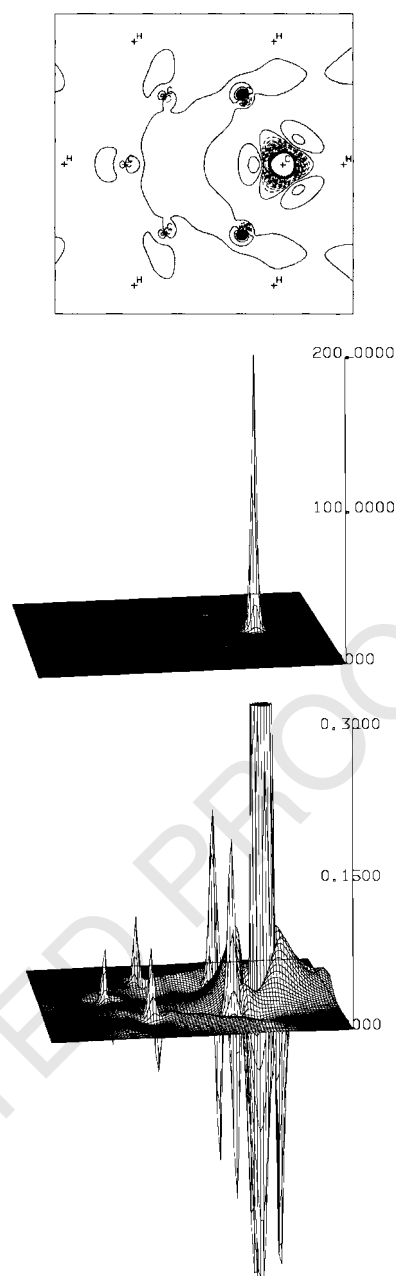


Figure 2. Carbon magnetic shielding density for Σ_{zz}^C on plane parallel to that of the benzene molecule, at a distance of 0.05 bohr. In the contour map, solid (dotted) lines mean positive (negative) values. In the contour map on top, the values of the solid (dashed) lines decrease (increase) in steps of $0.03 \text{ au} \times c^2$ (c is the velocity of light, $\sim 137.036 \text{ au}$) from the innermost contour. The maximum and minimum correspond to ~ 88.6 and $\sim -188.6 \text{ au} \times c^2$. To emphasize the contribution from distant carbons, the map in the center is expanded in the bottom plot. In this three-dimensional perspective view, magnetic shielding density values higher than 0.3 (smaller than -0.4) have been truncated.

61 Again, it is found that a sizeable contribution to carbon
 62 shielding is due to π electron circulation about *ortho*, *meta*
 63 and *para* carbons. The effect smoothly fades away in higher
 64 planes, but the contributions of π ring currents die off less
 65 rapidly than those arising from core and σ electrons. At large

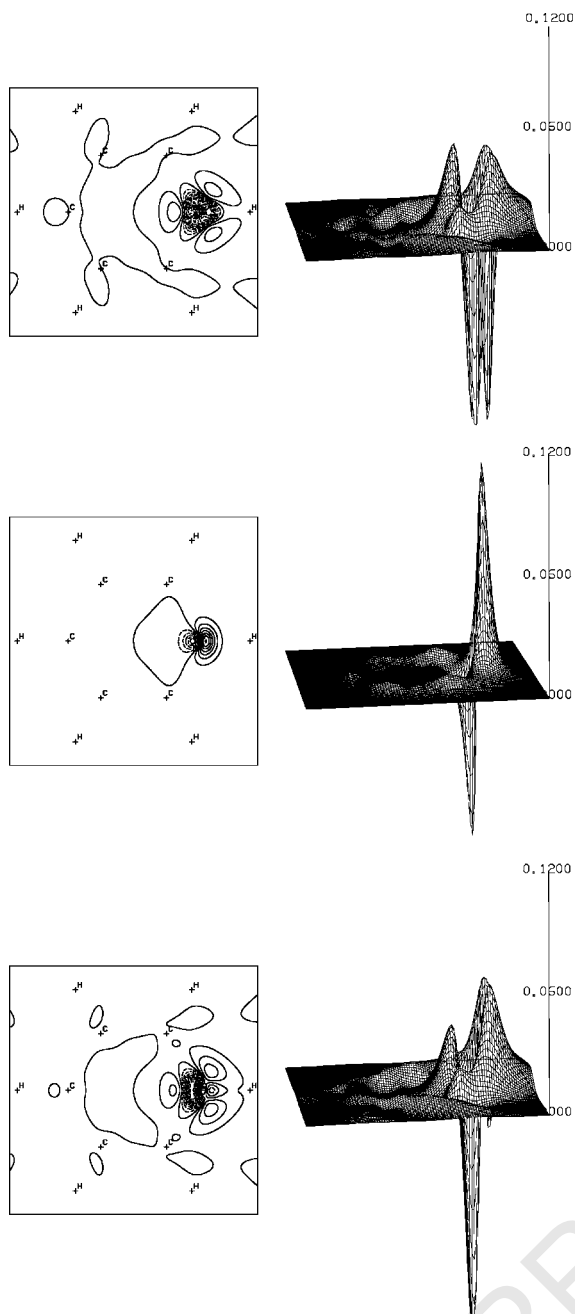


Figure 3. Carbon magnetic shielding density Σ_{ZZ}^C . In the contour maps on the left, solid (dotted) lines mean positive (negative) values. From top to bottom: contributions from core and σ orbitals, from π orbitals, and total values of Σ_{ZZ}^C . The plot plane is parallel to that of the molecule and displaced from it by 0.50 bohr. In the contour maps on the left, the values of the solid (dashed) lines decrease (increase) in steps of 1.5×10^{-2} au from the innermost contour. For the core and σ contributions, maximum and minimum values are at $\sim 4.1 \times 10^{-2}$ and ~ -0.11 au $\times c^2$, respectively. For the π contribution, the values of the maximum and minimum contour are ~ 0.107 and ~ -0.087 au $\times c^2$. For the total density, the values of the maximum and minimum contour are ~ 0.055 and ~ -0.131 au $\times c^2$.

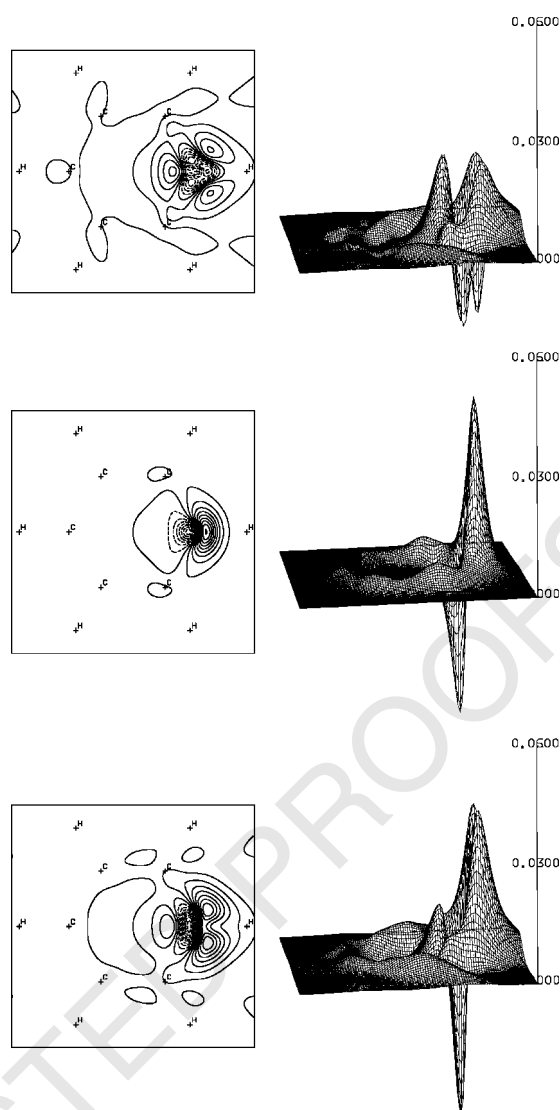


Figure 4. Carbon magnetic shielding density Σ_{ZZ}^C . From top to bottom: contributions from core and σ orbitals, from π orbitals, and total values of Σ_{ZZ}^C . The plot plane is parallel to that of the molecule and displaced from it by 0.75 bohr. In the contour maps on the left, the values of the solid (dashed) lines decrease (increase) in steps of 5.0×10^{-3} au from the innermost contour. For the core and σ contributions, maximum and minimum values are $\sim 2.2 \times 10^{-2}$ and $\sim -2.4 \times 10^{-2}$ au $\times c^2$, respectively. For the π contribution, maximum and minimum values are $\sim 4.5 \times 10^{-2}$ and $\sim -3.8 \times 10^{-2}$ au $\times c^2$, respectively. For the total density, the values of the maximum and minimum contour are $\sim 3.9 \times 10^{-2}$ and $\sim -4.2 \times 10^{-2}$ au $\times c^2$.

The partitioning of the out-of-plane component of carbon magnetic shielding confirms the predictions of the DBS relationship and earlier estimates:⁵ the positive contribution of π ring currents to σ_{\parallel}^C is ~ 19 ppm, which is 10% of the total value.

CONCLUSION

NMR practitioners have until recently had a consensus view that there were no specific ring current effects on

1 distance from the molecular plane, σ_{\parallel}^C is still biased by the
2 diamagnetic π flow.
3
4
5
6
7

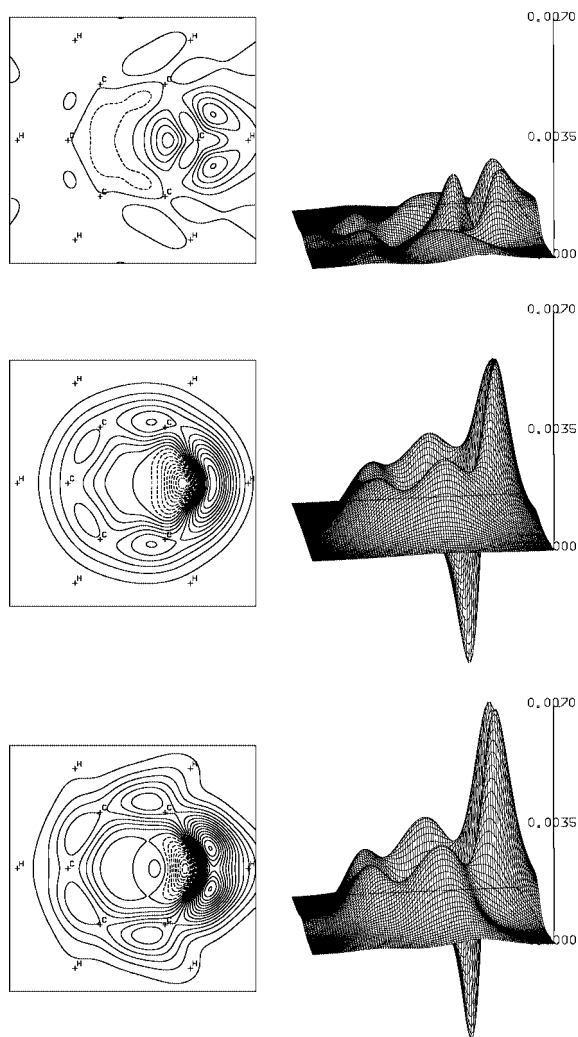


Figure 5. The conventions are the same as in Figs 3 and 4. The plot plane is parallel to that of the molecule and displaced from it by 1.5 bohr. In the contour maps on the left, the values of the solid (dashed) lines decrease (increase) in steps of 4.0×10^{-4} au from the innermost contour. For the core and σ contributions, maximum and minimum values are $\sim 2.0 \times 10^{-3}$ and $\sim -6.3 \times 10^{-3} \text{ au} \times c^2$, respectively. For the π contribution, maximum and minimum values are $\sim 5.0 \times 10^{-3}$ and $\sim -4.4 \times 10^{-3} \text{ au} \times c^2$, respectively. For the total density, the values of the maximum and minimum contour are $\sim 6.4 \times 10^{-3}$ and $\sim -3.8 \times 10^{-3} \text{ au} \times c^2$.

^{13}C , as opposed to ^1H , shifts. Despite previous calculations showing these effects,⁴ this apparently erroneous view prevailed owing to a lack of tools to interpret them. The DBS law¹⁴ and maps of the nuclear magnetic shielding density introduced by Jameson and Buckingham^{15,16} provide the fundamental instruments for analyzing the problem.^{7,11,12,13,22,23}

The quantum mechanical current density \mathbf{J} is the expectation value of a corresponding quantum mechanical operator, that is, a *sub-observable* in the terminology proposed by Hirschfelder.²⁹ This means that the $\mathbf{J}(\mathbf{r})$ field obtained via quantum procedures can be treated as a fully classical quantity. Therefore, the classical DBS law can be applied to develop reliable models for predicting the elemental

magnetic flux density induced at an observation point by different segments of a current loop.

The DBS relationship predicts that the out-of-plane component of the magnetic shielding of a reference carbon nucleus of benzene is unaffected by local π currents. However, its magnitude is enhanced by the π currents flowing in the domain of the other carbon atoms.

Maps of magnetic shielding density evaluated via the CTOCD-DZ2 coupled Hartree–Fock approximation allowing for extended basis sets confirm the practicality of the DBS-based model. The contribution of the π currents to the out-of-plane component of the shielding tensor at the carbon nucleus is $\sim 10\%$ of the total value.

We conclude that π ring currents are responsible for a minor but significant part of $\sigma_{\parallel}^{\text{C}}$ and hence of the observed anisotropy. This is in contrast to their effect on the molecular susceptibility and σ^{H} , where ring currents alone can account for the qualitative behavior of these quantities. Our finding shows that, although ring currents do play a role in determining the magnetic response of aromatic carbons, in order to understand the anisotropy of σ^{C} other interpretative models must be invoked or developed. It is our intention to engage this task in future publications.

Acknowledgments

Financial support for this work from the Proyecto del Programa de Cooperación Argentino–Italiana SECYT-MAE, código IT/PA03-EXII/082, the Italian MURST (Ministero dell'Università e della Ricerca Scientifica e Tecnologica), via 60% and FIRB funds, from the University of Buenos Aires (UBACYT X-035) and from the Argentinian CONICET is gratefully acknowledged.

REFERENCES

1. Appleman BR, Dailey BP. *Adv. Magn. Reson.* 1974; **7**: 231.
2. Englert G. *Z. Naturforsch., Teil A* 1972; **27**: 715.
3. Jameson AK, Jameson CJ. *Chem. Phys. Lett.* 1987; **134**: 461.
4. Fleischer U, Kutzelnigg W, Lazzarretti P, Mühlenkamp V. *J. Am. Chem. Soc.* 1994; **116**: 5298.
5. Lazzarretti P. *Prog. Nucl. Magn. Reson. Spectrosc.* 2000; **36**: 1.
6. Ligabue A, Soncini A, Lazzarretti P. *J. Am. Chem. Soc.* 2002; **124**: 2008.
7. Ferraro MB, Lazzarretti P, Viglione RG, Zanasi R. *Chem. Phys. Lett.* 2004; **390**: 268.
8. Viglione RG, Zanasi R, Lazzarretti P. *Org. Lett.* 2004; **6**: 2265.
9. Lazzarretti P. *Phys. Chem. Chem. Phys.* 2004; **6**: 217.
10. Wannere CS, Schleyer PvR. *Org. Lett.* 2003; **5**: 605.
11. Soncini A, Fowler PW, Lazzarretti P, Zanasi R. *Chem. Phys. Lett.* Submitted.
12. Pelloni S, Ligabue A, Lazzarretti P. *Org. Lett.* 2004; ASAP article on the web.
13. Cuesta IG, Ligabue A, de Merás AS, Lazzarretti P. *Chem. Phys. Lett.* Submitted.
14. Jackson JD. *Classical Electrodynamics* (3rd edn). Wiley: New York, 1999; 175.
15. Jameson CJ, Buckingham AD. *J. Phys. Chem.* 1979; **83**: 3366.
16. Jameson CJ, Buckingham AD. *J. Chem. Phys.* 1980; **73**: 5684.
17. Lazzarretti P, Malagoli M, Zanasi R. *Chem. Phys. Lett.* 1994; **220**: 299.
18. Johnson CE, Bovey FA. *J. Chem. Phys.* 1958; **29**: 1012.
19. Waugh JS, Fessenden RW. *J. Am. Chem. Soc.* 1958; **80**: 6697.
20. Farnum DG, Wilcox CF. *J. Am. Chem. Soc.* 1967; **89**: 5379.
21. Lazzarretti P. in *Handbook of Molecular Physics and Quantum Chemistry*, vol. 3, Part 1, Wilson S (ed). Wiley: Chichester, 2003; Chapt. 3, 53.
22. Lazzarretti P, Zanasi R. *Chem. Phys. Lett.* 1983; **100**: 67.

1	23. Keith TA, Bader RFW. <i>Can. J. Chem.</i> 1996; 74 : 185.	27. Zanasi R. <i>J. Chem. Phys.</i> 1996; 105 : 1460.	33
2	24. Sauer SPA, Paidarová I, Oddershede J. <i>Mol. Phys.</i> 1994; 81 : 87.	28. Lazzarotti P, Malagoli M, Zanasi R. <i>J. Chem. Phys.</i> 1995; 102 : 9619.	34
3	25. Diercksen G, McWeeny R. <i>J. Chem. Phys.</i> 1966; 44 : 3554.	29. Hirschfelder JO. <i>J. Chem. Phys.</i> 1978; 68 : 5151.	35
4	26. Keith TA, Bader RFW. <i>Chem. Phys. Lett.</i> 1993; 210 : 223.		36
5			37
6			38
7			39
8			40
9			41
10			42
11			43
12			44
13			45
14			46
15			47
16			48
17			49
18			50
19			51
20			52
21			53
22			54
23			55
24			56
25			57
26			58
27			59
28			60
29			61
30			62
31			63
32			64

UNCORRECTED PROOFS

1		61
2	QUERIES TO BE ANSWERED BY AUTHOR	62
3		63
4	IMPORTANT NOTE: Please mark your corrections and answers to these queries directly onto the proof at the relevant	64
5	place. Do NOT mark your corrections on this query sheet.	65
6		66
7	Queries from the Copyeditor:	67
8	AQ1 Are the keywords OK?	68
9	AQ2 "In Eqn (2)" correct?	69
10	AQ3 Eqn (1)-correct?	70
11	AQ4 Figs 2–5: correct?	71
12	AQ5 Update?	72
13	AQ6 Please give published ref. if available.	73
14	AQ7 Update?	74
15		75
16		76
17		77
18		78
19		79
20		80
21		81
22		82
23		83
24		84
25		85
26		86
27		87
28		88
29		89
30		90
31		91
32		92
33		93
34		94
35		95
36		96
37		97
38		98
39		99
40		100
41		101
42		102
43		103
44		104
45		105
46		106
47		107
48		108
49		109
50		110
51		111
52		112
53		113
54		114
55		115
56		116
57		117
58		118
59		119
60		120